ADVANCED MATERIALS

rise to strong π–π interactions, and hence induces more stable columnar phases[13] and gelling ability. The formation of columnar molecular assemblies through macroscopic phase separation plays a crucial role in the gelling process.[14]

Experimental

Materials: Compounds **5**–**9** were prepared by the reaction of 5-cyanotropolone, 2-amino-5-cyanotropone, and 2-aminomethyl-5-cyanotropone, respectively, with 3,4,5-trialkoxybenzoyl chloride. Elemental analyses and spectral data of the new compounds were satisfied, and details are available from the authors.

ESEM: Environmental scanning electron microscope (ESEM) images of dried gels in hexane and of octanol gels (3 wt.-%) were taken with a Nikon ESEM-2700 under water with a pressure of 200 Pa for dried gels and 480 Pa for octanol gels.

Characterization: X-ray diffraction analysis was undertaken using a Rigaku Rint 2100 system and Ni-fillered Cu-Kα radiation. A polarizing microscope (Olympus BHSP BH-Z microscope equipped with a Linkam TH-600RMS hotstage) was used for optical characterization.

Received: May 15, 2002
Final version: December 10, 2002

[1] *Handbook of Liquid Crystals* (Eds: D. Demus, J. Goodby, G. W. Gray, H.-W. Spiess, V. Vill), Wiley-VCH, Weinheim **1998**.
[2] a) T. Tachibana, T. Mori, K. Hori, *Bull. Chem. Soc. Jpn*. **1980**, *53*, 1714. b) K. Hanabusa, M. Yamada, M. Kimura, H. Shirai, *Angew. Chem. Int. Ed. Engl.* **1996**, *35*, 1949. c) M. de Loos, J. van Esch, I. Stokroos, R. M. Kellogg, B. L. Feringa, *J. Am. Chem. Soc.* **1997**, *119,* 12 675. d) K. Yoza, Y. Ono, K. Yoshihara, T. Akao, H. Shinmori, M. Takeuchi, S. Shinkai, D. N. Reihoudt, *Chem. Commun.* **1998**, 907. e) V. P. Vassilev, E. E. Simanek, M. R. Wood, C.-H. Wong, *Chem. Commun.* **1998**, 1865. f) R. Oda, I. Huc, S. J. Candau, *Angew. Chem. Int. Ed.* **1998**, *37*, 2689. g) P. Trech, J. J. Allegrand, C. M. Gerner, *Langmuir* **1998**, *14*, 3991. h) A. J. Carr, R. Melendoz, S. J. Geib, A. D. Hamilton, *Tetrahedron Lett.* **1998**, *39*, 7447. i) K. Hanabusa, M. Maesaka, M. Kimura, H. Shirai, *Tetrahedron Lett.* **1999**, *40*, 2385. j) F. Placin, J.-P. Desvergne, F. Cansell, *J. Mater. Chem.* **2000**, *10*, 2147. k) D. J. Abdallah, R. D. Weiss, *Adv. Mater.* **2000**, *12*, 1237. l) X. Luo, C. Li, Y. Liang, *Chem. Commun.* **2000**, 2091. m) K. Hanabusa, Y. Maesaka, M. Suzuki, M. Kimura, H. Shirai, *Chem. Lett.* **2000**, 1168. n) J. H. Jung, Y. Ono, K. Hanabusa, S. Shinkai, *J. Am. Chem. Soc.* **2000**, *122*, 5008. o) M. Kölbel, F. M. Menger, *Chem. Commun.* **2001**, 275.
[3] a) A. Mori, H. Takeshita, K. Kida, M. Uchida, *J. Am. Chem. Soc.* **1990**, *112*, 8635. b) A. Mori, N. Kato, H. Takeshita, M. Uchida, H. Taya, R. Nimura, *J. Mater. Chem.* **1991**, *1*, 799. c) A. Mori, H. Takeshita, R. Nimura, M. Isobe, *Liq. Cryst.* **1993**, *14*, 821. d) A. Mori, H. Taya, M. Uchida, H. Takeshita, *Chem. Lett.* **1996**, 699. e) A. Mori, H. Taya, H. Takeshita, S. Ujiie, *J. Mater. Chem.* **1998**, *8*, 595. f) M. Takemoto, A. Mori, S. Ujiie, *Chem. Lett.* **1999**, 1177. g) A. Mori, H. Takeshita, R. Mori, S. Takematsu, M. Takemoto, S. Ujiie, *Liq. Cryst.* **2001**, *28*, 171.
[4] M. Hashimoto, S. Ujiie, A. Mori, *Chem. Lett.* **2000**, 758.
[5] a) C. F. van Nostrum, S. J. Picken, A.-J. Schouten, R. J. M. Nolte, *J. Am. Chem. Soc.* **1995**, *117*, 9957. b) S. Ito, P. T. Herwig, T. Böhme, J. P. Rabe, W. Rettig, K. Müllen, *J. Am. Chem. Soc.* **2000**, *122*, 7698.
[6] a) U. Beginn, S. Keinath, M. Möller, *Liq. Cryst.* **1997**, *23*, 35. b) U. Beginn, S. Keinath, M. Möller, *Macromol. Chem. Phys., Suppl.* **1998**, *199*, 2379.
[7] K. Borisch, S. Diele, P. Göring, H. Kresse, C. Tschierske, *J. Mater. Chem.* **1998**, *8*, 529.
[8] D. J. Stokes, *Adv. Eng. Mater.* **2001**, *3*, 126.
[9] a) K. Sakurai, T. Kimura, O. Gronwald, K. Inoue, S. Shinkai, *Chem. Lett.* **2001**, 746. b) C. Kim, K. T. Kim, Y. Chang, *J. Am. Chem. Soc.* **2001**, *123*, 5586.
[10] a) A. Mori, K. Katahira, K. Kida, H. Takeshita, *Chem. Lett.* **1992**, 1767. b) A. Mori, H. Takeshita, K. Katahira, K. Kida, C. Jin, S. Ujiie, *Liq. Cryst*. **2002**, *29*, 1235.
[11] A. Mori, K. Hirayama, N. Kato, H. Takeshita, S. Ujiie, *Chem. Lett.* **1997**, 509.
[12] A. Mori, N. Kato, H. Takeshita, R. Nimura, M. Isobe, C. Jin, S. Ujiie, *Liq. Cryst.* **2001**, *28*, 1425
[13] a) A. R. A. Palmans, J. A. J. M. Vekemans, H. Fischer, R. A. Hikmet, E. W. Meijer, *Chem. Eur. J.* **1997**, *3*, 300. b) A. R. A. Palmans, J. A. J. M. Vekemans, R. A. Hikmet, H. Fischer, E. W. Meijer, *Adv. Mater*. **1998**, *10*, 873. c) W. Shu, S. Valiyaveettil, *Chem. Commun.* **2002**, 1350.
[14] U. Beginn, G. Zipp, M. Möller, *Chem. Eur. J.* **2000**, *6*, 2016.

Organic Light-Emitting Devices Fabricated from Semiconducting Nanospheres**

By *Thomas Piok*, *Stefan Gamerith*, *Christoph Gadermaier*, *Harald Plank*, *Franz P. Wenzl*, *Satish Patil*, *Rivelino Montenegro*, *Thomas Kietzke*, *Dieter Neher*,* *Ullrich Scherf*,* *Katharina Landfester*,* and *Emil J. W. List**

The trend towards nanoscale organic electronics raises the quest for novel materials and concepts that allow control of the deposition of the active material on the nano- to mesoscopic scale. Gaining control over the material at such a scale will enable the fabrication of novel as well as improved devices from organic semiconductors such as conjugated polymers in a cost-effective way. As demonstrated over the last decade, conjugated polymers can be utilized as the active medium in organic light-emitting diodes (OLEDs),[1] light-emitting electrochemical cells (LECs),[2] solar cells,[3] photo detectors,[4] lasers,[5] field-effect transistors,[6] and all-polymer integrated electronic circuits.[7]

By adopting the so-called miniemulsion process one can combine the properties of semiconducting polymers with those of nanostructured matter, as has been shown recently.[8] Miniemulsions are understood as stable emulsions of droplets with a distinct size of 50–500 nm, made by shearing a system containing water, a solution of a highly water insoluble compound (hydrophobe, e.g., a polymer), and a small amount of a surfactant.[9] Polymer particles can be obtained from such droplets after evaporation of the solvent. Using such an approach semiconducting conjugated polymer nanospheres (SPNs) dispersed in water have been produced successfully.[10] This novel approach enables the application of environmen-

[*] Dr. E. J. W. List, T. Piok, S. Gamerith, Dr. C. Gadermaier, H. Plank
Christian Doppler Laboratory Advanced Functional Materials
Institute of Solid State Physics, Graz University of Technology
Petersgasse 16, A-8010 Graz (Austria)
and
Christian Doppler Laboratory Advanced Functional Materials
Institute of Nanostructured Materials and Photonics
Franz-Pichler-Strasse 30, A-8160 Weiz (Austria)
E-mail: e.list@tugraz.at
F. P. Wenzl
Institute of Solid State Physics, Graz University of Technology
Petersgasse 16, A-8010 Graz (Austria)
Prof. U. Scherf, S. Patil
Department of Chemistry, BUGH Wuppertal
Gauss-Str. 20, D-42097 Wuppertal (Germany)
E-mail: scherf@uni-wuppertal.de
Dr. K. Landfester, Dr. R. Montenegro
Max Planck Institute of Colloids and Interfaces
Research Campus Golm
D-14424 Potsdam (Germany)
E-mail: landfester@mpikg-golm.mpg.de
Prof. D. Neher, T. Kietzke
Institute of Physics, University of Potsdam
Am Neuen Palais 10, D-14469 Potsdam (Germany)
E-mail: neher@rz.uni-potsdam.de

[**] The authors acknowledge financial support from TMR EUROLED, and the Austrian FWF project P14170-TPH. CDL-AFM is a key member of the long term AT&S research activities. Supporting information is available from the authors upon request.

  DOI: 10.1002/adma.200304253

tally friendly water-based deposition techniques such as ink-jet printing and opens new ways to controlled multilayer formation, simply by using one of the materials as an aqueous SPN dispersion.[10] Moreover, aqueous SPN dispersions facilitate sol–gel processing[11] and may be used for the generation of SPN-based photonic crystals,[12] e.g., via self assembly techniques.

The application of SPNs to optoelectronic applications requires, however, that neither the formation of the SPNs nor the deposition and film formation alters the electronic and structural properties of the semiconducting polymers. This question requires careful investigations, since the preparation of the miniemulsions involves the application of strong ultrasonic shear. Yet, as a first step towards SPN-based devices we have built OLEDs with a SPN-active layer. In this study we report on the characteristics of such SPN single-layer OLEDs and compare them to OLEDs fabricated by a common spin-coating process from organic solvents.

It has been demonstrated that the optoelectronic properties of conjugated polymers, such as the photoluminescence (PL) and PL quantum yield, are extremely sensitive to chemical defects,[13] impurities,[14] and solid-state packing effects.[15] Hence, the properties of SPNs of different sizes, ranging from 69–154 nm, have been characterized carefully by means of optical spectroscopy.

In Figure 1 the emission and absorption spectra of an SPN dispersion based on a methyl-substituted ladder-type poly(*para*-phenylene) (m-LPPP)[16] (see inset of Fig. 1 for chemical structure) are compared to those of a dilute m-LPPP solution (toluene) and spin-coated films; all prepared from an identical batch of m-LPPP.

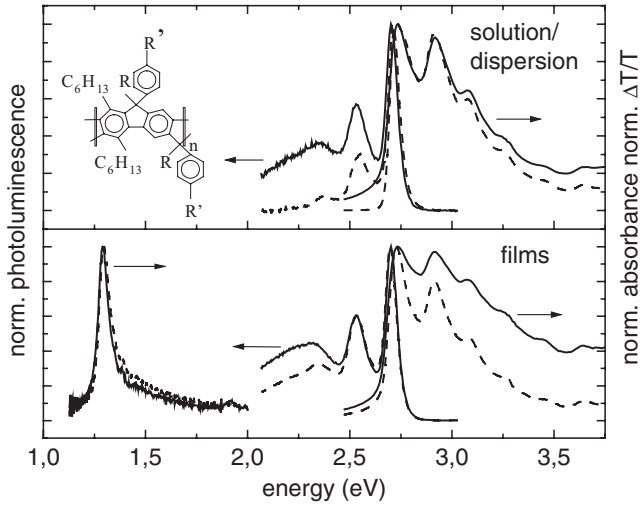

Fig. 1. Top, right: Normalized photoluminescence and absorbance spectra of a dilute solution of m-LPPP in toluene (dashed lines), and normalized photoluminescence and absorbance of the SPN (m-LPPP) dispersion in water (solid lines). Top, left: Chemical structure of m-LPPP. Bottom, right: Normalized photoluminescence and absorbance spectra of a m-LPPP film (dashed lines), and normalized photoluminescence and absorbance spectra of an SPN film (solid lines). Bottom, left: Photoinduced absorption of a m-LPPP film (triplet exciton absorption at an energy of 1.3 eV, solid line) and of a m-LPPP colloid film (triplet exciton absorption at an energy of 1.3 eV, dashed line)

Note that the emission and absorption spectra of SPN dispersions of different particle sizes do not reveal significant differences, i.e., the optical properties of the particles are not size dependent. SPN dispersion, SPN film, and "common" m-LPPP, both in solution and the solid state, display no significant differences in their spectra. All emission spectra are characterized by a steep onset at 2.7 eV accompanied by well-resolved vibronic side bands; they are a mirror image of the absorption spectrum as discussed in detail elsewhere.[17]

The nearly identical absorption spectra of m-LPPP in dispersion and solution—despite the high dielectric constant of water[18]—show that there is no significant interaction between the SPNs and the surrounding water. The tailing of the thin-film absorption spectra originates from scattering effects.

Yet, although the emission spectrum of m-LPPP-based SPNs in aqueous dispersion basically resembles that of a dilute m-LPPP solution (toluene) the spectra slightly differ as a consequence of the solid-state nature of the polymeric SPNs. The 0–1 (2.52 eV) as well as 0–2 vibronic replica become more dominant due to weak solid-state interactions of the polymer chains,[19] which can also account for the observed slight PL red shift of the SPN dispersion in comparison to a toluene solution. Moreover, a low-energy tail due to an enhanced energy transfer to defect sites (as also known for thin films of the polymer)[20] can be observed in the PL spectrum of the SPN dispersion.[21] Spin- or drop-casting the aqueous SPN dispersions yields thin layers whose emission properties are not altered.

No significant differences in the solid-state quantum yields have been observed for bulk and SPN layers. The photoinduced absorption spectrum, which indicates defect-stabilized excited states,[14] such as polarons, shows a very similar shape and relative intensities for bulk and SPN-based films. This provides evidence that no additional electronic defects are incorporated upon processing of m-LPPP into SPNs. In both spectra the triplet absorption is observed at 1.3 eV, while a weak trace of the polaronic absorption is located at 1.9 eV.

For optoelectronic investigations homogeneous single layers of closely packed SPNs with a layer thickness given by the diameter of the particles (see the atomic force microscopy (AFM) image in Fig. 2) were spin-coated onto ITO-coated glass substrates supported with a very thin poly(3,4-ethylenedioxythiophene)/poly(styrene sulfonate) (PEDOT/PSS) layer. It is known from the literature that the quality of nanosphere layers prepared from aqueous dispersion strongly depends on the wetting of the substrate, the spinning speed, and the concentration of the dispersion.[22] For low spinning speeds the film consists of domains of multilayers with an irregular variation of the thickness across the sample surface. If the spinning speed is too high, a monolayer is formed but the coverage of the substrate will not be complete. However, within a certain speed range a continuous monolayer of closely packed particles can be deposited. Within this speed range deposition of SPNs from aqueous phase always results in monolayer coverage with a defined thickness. This behavior is common to all the SPN particle sizes investigated.[23] Optical microscopy cer-

ADVANCED MATERIALS

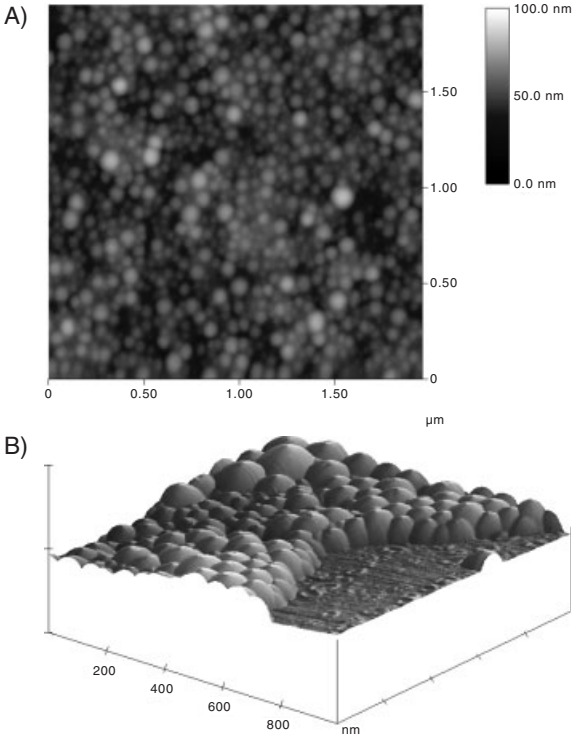

Fig. 2. A) AFM height image (tapping mode) of an SPN monolayer on a glass substrate. B) 3D AFM image of an SPN monolayer on a glass substrate, where part of the material has been removed.

tifies that the films are very homogeneous over an area of typically more than 5 mm × 5 mm. Atomic force microscopy reveals no cracks in the closely packed SPN layers and a root mean square (rms) roughness of less than 15 nm for SPNs of 94 nm diameter (not shown).

Removing part of an SPN-based film composed of 94 nm particles by scratching revealed a total step height of 85 nm using the Tolansky technique, independent of whether the glass/ITO substrate had been coated with PEDOT/PSS or not. A parallel AFM investigation of the SPN films on glass provided a step height of ca. 83 nm (not shown). This observation can be explained by the fact that the PEDOT/PSS layer with a typical thickness of 60–100 nm is almost completely removed during the deposition of the SPNs from aqueous dispersion. This assumption has been verified by spin-coating pure water onto PEDOT/PSS films and determining the residual film thickness. Investigations of the single-layer homogeneity by comparing several films deposited on pristine substrates and substrates bearing a PEDOT/PSS layer confirmed better film formation on PEDOT/PSS-coated substrates. Therefore, the PEDOT/PSS films may assist monolayer film formation.

As depicted in Figure 3, devices fabricated from m-LPPP SPNs with a mean diameter of ca. 94 nm exhibit light emission with a current onset at the SPN energy gap (ca. 2.7 eV for m-LPPP) in the forward bias direction and a maximum brightness of ca. 145 cd m^{-2} at 8 V. The emission occurs homogeneously across the layer, reflecting the homogeneous coverage with nanoparticles. This electrical characteristic is independent of the presence of an additional PEDOT layer. The low electroluminescence (EL) onset of the SPN OLEDs in forward bias direction is surprising, especially in relation to "common" OLEDs fabricated from m-LPPP solutions by spin-coating (see Fig. 3C). Such OLEDs exhibit an EL onset at ca. 7 V in forward bias direction.

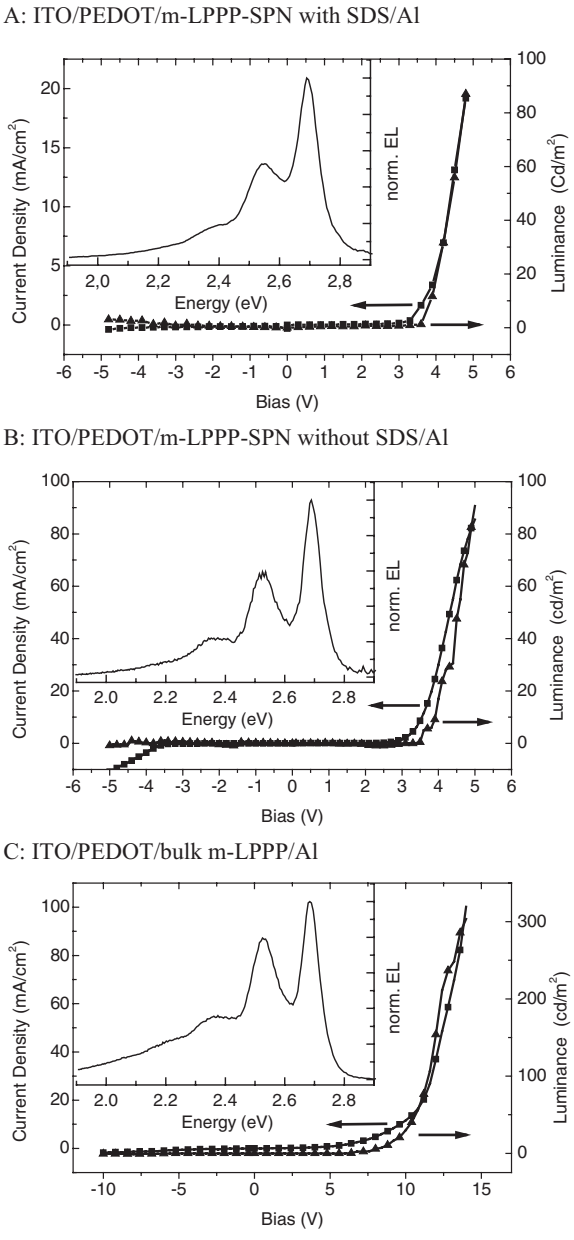

Fig. 3. A) *I–V* (squares) and *L–V* (triangles) characteristics of an OLED prepared from m-LPPP SPNs with a mean diameter of ca. 94 nm. The inset shows the electroluminescence emission spectrum of the OLED at a bias of 5 V. B) *I–V* (squares) and *L–V* (triangles) characteristics of an OLED prepared from dialyzed m-LPPP SPNs with a mean diameter of ca. 125 nm. The inset shows the electroluminescence emission spectrum of the OLED at a bias of 5 V. C) *I–V* (squares) and *L–V* (triangles) characteristics of an OLED with a bulk m-LPPP layer, prepared from solution. The inset shows the electroluminescence emission spectrum of the OLED at a bias of 12 V.

In order to check the influence of the small amount of surfactant (sodium dodecyl sulfate (SDS)) used in the SPN preparation[8] on the OLED performance, devices based on care-

fully dialyzed SPNs (i.e., the surfactant had been removed) were also fabricated and tested as depicted in Figure 3B. The surfactant could cause some electrochemical doping of the polymer during operation, subsequently lowering the onset voltage as observed in light-emitting electrochemical cells (LECs)[2] or a space–charge assisted charge injection as suggested by de Mello et al.[24] Both devices show the same onset and almost the same EL characteristics, thus one can conclude that such ion-mediated effects, if present, have only a minor influence. Moreover, both kinds of devices reveal a very similar maximum brightness of up to 145 cd m^{-2} at 8 V. On the other hand, several devices prepared from dialyzed SPN dispersions suffered shorts that are related to pinholes as observed by optical microscopy. This behavior clearly classifies SPN dispersions containing residual SDS above dialyzed SPN dispersions. Yet, to achieve further improvements in the film formation behavior of SPN dispersions different surfactants will be used and tested.

Since the low turn-on voltage of the SPN-based OLEDs can be predominately assigned neither to the PEDOT layer nor to the presence of ionic species, we attribute the significant onset reduction of the SPN-based devices to an enhanced electron injection from the cathode. Note that onsets as low as 3 V in m-LPPP OLEDs can normally be achieved only by applying low work function cathodes such as calcium.[25] We therefore propose that the observed low onset is caused by an enhanced local electric field resulting from the "stalactite"-type, nanostructured aluminum cathodes. Such structured electrodes are formed when the Al cathode is deposited on top of the rough surface of the SPN monolayer. We note that a similar effect was observed by Yang et al. utilizing high surface area hole-injection electrodes fabricated from polyaniline.[26] The high local electric field caused by the rough polyaniline electrode resulted in lower voltage operation and higher efficiency of the devices investigated. Typical devices fabricated from SPNs also exhibited a slightly better device efficiency of ca. 0.5 cd A^{-1} compared to "traditionally" fabricated m-LPPP-based OLEDs (0.3 cd A^{-1}). All devices show color stable and reproducible *I–V* and *L–V* characteristics over the characterization period of a few hours. No further testing for stability of the devices has been undertaken.

In addition to the above-presented SPN OLEDs with an emission layer of shape-persistent m-LPPP particles, OLEDs have also been prepared from SPNs of low glass transition temperature (T_g) polymers. In this case, the particles already coalesce during film formation at room temperature and flat polymer layers can be realized. This approach can be further exploited for the build-up of smooth multilayer structures with defined interfaces. For LED fabrication, we used SPNs prepared from poly(9,9-bis(3,7,11-trimethyldodecyl)fluorene) (PF111/12), a polyfluorene derivative with a T_g close to room temperature. As described recently, individual particles cannot be detected after film formation from PF111/12 SPNs.[8] These layers are rather homogeneous and withstand quite large current densities of more than 100 mA cm^{-2} without breakdown and single-layer OLED devices based on SPN films of this PF derivative show similar brightness to that observed for m-LPPP SPN devices.

In conclusion, we report for the first time the successful fabrication of OLEDs utilizing organic semiconducting polymer nanospheres. The devices consist of a homogeneous single layer of nanosized SPNs and reveal improved opto-electronic characteristics (lower onset, slightly higher efficiency) compared with "traditionally" fabricated OLEDs for which the active layer is cast from a solution of the conjugated polymer in an organic solvent. We attribute this behavior to an enhanced electron injection from the cathode as a consequence of in-situ formation of a "stalactite"-type nanostructured cathode during aluminum evaporation. Optical spectroscopy has evidenced that conjugated polymers can be converted into aqueous SPN dispersions without generation of electronic defects; the SPNs display the photophysical properties of the bulk polymer.

However, the enhancement of the local electric field in the SPN-based OLEDs also introduces local stress and may cause device failure at higher voltages. Nevertheless, the SPN concept may be a first step towards a novel variety of nanoscale organic electronics.

Experimental

The preparation of the SPNs is described in detail in the literature [8] as is the synthesis of the utilized conjugated polymers m-LPPP and PF111/12 [16,24]. Commercially available ITO-coated glass substrates were cleaned in a series of different organic solvents and treated with chromosulfuric acid. PEDOT/PSS as purchased from Bayer (Baytron P) was spin-coated and dried according to the specifications of the distributor. Afterwards the SPN dispersions were spin-coated, and the films were dried in an oven for about 15 min at 75 °C. The thickness of the SPN layers was verified by optical absorption measurements, atomic force microscopy (DI Nanoscope Dimension 3100, tapping mode), and Tolansky measurements. A Balzers MED010 vacuum coating unit was used to deposit the aluminum top electrodes at a base pressure of 4×10^{-6} mbar. The different devices were fabricated under identical experimental conditions and operated in house-made sample holders in argon atmosphere. The current/luminance/voltage (*I*/*L*/*V*) characteristics were recorded in a customized setup using a Keithley 236 source measure unit for recording the current/voltage characteristics while the luminance characteristics were recorded using a calibrated photodiode attached to an integrating sphere. Electroluminescence spectra were recorded using an ORIEL charge coupled device (CCD) spectrometer. UV-vis transmission spectra were measured using a Perkin-Elmer λ9 spectrophotometer. PL emission spectra were recorded using a Shimadzu RF5301 spectrofluorometer. For the photoinduced absorption measurements the samples were mounted in a cryostat and cooled to a temperature of 80 K. As transmission source we used a standard 160 W halogen lamp. As excitation source an Ar^+ laser operated in the multiline UV mode (3.64 eV, 3.42 eV) was used. The lifetimes of the triplet excitons were determined by modulation spectroscopy from frequency-dependent photoinduced absorption measurements at an energy of 1.3 eV.

Received: July 31, 2002
Final version: February 6, 2003

[1] a) R. H. Friend, R. W. Gymer, A. B. Holmes, J. H. Burroughes, R. N. Marks, C. Taliani, D. D. C. Bradley, D. A. Dos Santos, J. L. Brédas, M. Lögdlund, W. R. Salaneck, *Nature* **1999**, *397*, 121. b) J. H. Burroughes, D. D. C. Bradley, A. R. Brown, R. N. Marks, K. Mackay, R. H. Friend, P. L. Burn, A. B. Holmes, *Nature* **1990**, *347*, 539.

[2] a) Q. Pei, G. Yu, C. Zhang, Y. Yang, A. J. Heeger, *Science* **1995**, *269*, 1086. b) L. Holzer, F. P. Wenzl, S. Tasch, G. Leising, B. Winkler, L. Dai, A. Mau, *Appl. Phys. Lett.* **1999**, *75*, 2014.

[3] a) N. S. Sariciftci, L. Smilowitz, A. J. Heeger, F. Wudl, *Science* **1992**, *258*, 1474. b) M. Granström, K. Petritsch, A. C. Arias, A. Lux, M. R. Andersson, R. H. Friend, *Nature* **1998**, *395*, 257.

ADVANCED MATERIALS

[4] G. Yu, J. Gao, J. C. Hummelen, F. Wudl, A. Heeger, *Science* **1995**, *270*, 1789.
[5] a) S. Stagira, M. Zavelani-Rossi, M. Nisoli, S. DeSilvestri, G. Lanzani, C. Zenz, P. Mataloni, G. Leising, *Appl. Phys. Lett*. **1998**, *73*, 2860. b) C. Kallinger, M. Hilmer, A. Haugeneder, M. Perner, W. Spirkl, U. Lemmer, J. Feldmann, U. Scherf, K. Müllen, A. Gombert, V. Wittwer, *Adv. Mater.* **1998**, *10*, 920.
[6] F. Garnier, R. Hajlaoui, A. Yassar, P. Srivastava, *Science* **1994**, *265*, 1684.
[7] P. K. H. Ho, D. S. Thomas, R. H. Friend, N. Tessler, *Science* **1999**, *285*, 233.
[8] K. Landfester, R. Montenegro, U. Scherf, R. Güntner, U. Asawapirom, S. Patil, D. Neher, T. Kietzke, *Adv. Mater*. **2002**, *14*, 651.
[9] K. Landfester, *Macromol. Rapid Commun.* **2001**, *22*, 896.
[10] K. Landfester, *Adv. Mater*. **2001**, *13*, 765.
[11] W.-P. Chang, W.-T. Whang, *Polymer* **1996**, *37*, 4229.
[12] Z. Cheng, W. B. Russel, P. M. Chaikin, *Nature* **1999**, *401*, 893.
[13] a) M. Yan, L. J. Rothberg, F. Papadimitrakopoulos, M. E. Galvin, T. M. Miller, *Phys. Rev. Lett*. **1994**, *73*, 744. b) U. Scherf, E. J. W. List, *Adv. Mater*. **2002**, *14*, 477.
[14] a) E. J. W. List, C. H. Kim, J. Shinar, A. Pogantsch, G. Leising, W. Graupner, *Appl. Phys. Lett.* **2000**, *76*, 2083. b) E. J. W. List, C.-H. Kim, A. K. Naik, U. Scherf, G. Leising, W. Graupner, J. Shinar, *Phys. Rev. B* **2001**, *64*, 155 204. c) J. M. Lupton, A. Pogantsch, T. Piok, E. J. W. List, S. Patil, U. Scherf, *Phys. Rev. Lett.* **2002**, *89*, 167 401.
[15] M. Pope, C. E. Swenberg, *Electronic Processes in Organic Crystals and Polymers*, 2nd ed., Oxford University Press, New York **1999**.
[16] U. Scherf, K. Müllen, *Makromol. Chem. Rapid Commun.* **1991**, *12*, 489.
[17] S. Tasch, G. Kranzelbinder, G. Leising, U. Scherf, *Phys. Rev. B* **1997**, *55*, 5079.
[18] J. R. Lakowicz, *Principles of Fluorescence Spectroscopy*, Plenum Press, New York **1983**.
[19] E. J. W. List, C. Creely, G. Leising, N. Schulte, A. D. Schlüter, U. Scherf, K. Müllen, W. Graupner, *Chem. Phys. Lett.* **2000**, *325*, 132.
[20] E. J. W. List, R. Guentner, P. Scandiucci de Freitas, U. Scherf, *Adv. Mater.* **2002**, *14*, 374.
[21] T. Piok, F. P. Wenzl, C. Gadermaier, U. Scherf, K. Landfester, E. J. W. List, unpublished.
[22] H. W. Deckman, J. H. Dunsmuir, *Appl. Phys. Lett.* **1982**, *41*, 377.
[23] For no particular reason SPN with a diameter of approx. 94 nm for m-LPPP and 74 nm for PF11112 has been used for the preparation of the OLEDs.
[24] J. C. de Mello, N. Tessler, S. C. Graham, R. H. Friend, *Phys. Rev. B* **1998,** *57*, 12 951.
[25] V. Bliznyuk, B. Ruhstaller, P. J. Brock, U. Scherf, S. A. Carter, *Adv. Mater.* **1999**, *11*, 1257.
[26] Y. Yang, E. Westerweele, C. Zhang, P. Smith, A. J. Heeger, *J. Appl. Phys.* **1995**, *77*, 694.

Benchtop Fabrication of Submicrometer Metal Line and Island Arrays Using Passivative Microcontact Printing and Electroless Plating**

By *Cristin E. Moran*, *Corey Radloff*, and *Naomi J. Halas**

The controlled fabrication of two- and three-dimensionally (3D) ordered structures is important for the nanoengineering of materials and devices.[1–3] In particular, metal nanostructures are increasingly important building blocks for new materials due to their shape-dependent plasmon response and thus their tunable optical properties.[4–8] The emergent field of plasmonics is particularly concerned with how surface plasmons propagate, localize, or interact on metal nano- and microstructures. Exploitation of surface plasmon propagation in these regimes can be used to develop new devices in nano-optics and optical computing,[9] waveguides,[10] biomolecular, and chemical sensor arrays,[11] optical filters,[12] and surface-enhanced Raman substrates.[13,14]

Our goal is to fabricate arrays of discrete metal nanostructures which can be easily varied in size and shape, and are replicated over large areas, on an optically transparent substrate. Microcontact printing, a form of soft lithography, is a non-photolithographic technique in which molecular patterns are transferred to surfaces using a polydimethylsiloxane (PDMS) stamp.[15,16] The polymer stamp is molded from a master template, which is the relief of the desired printed pattern, and is wetted by a solution of the molecule to be transferred. This technique is fast, simple, and inexpensive and has inspired several new fabrication methods. Other groups have previously fabricated planar metal structures using microcontact printing.[17] Whitesides and co-workers have developed a method which involves stamping a pattern of protective alkanethiols onto a metal surface and using a chemical etch to remove the non-stamped regions.[18–22] A second method uses a PDMS stamp to transfer palladium colloid directly to a surface onto which copper is deposited by electroless plating.[23] Others have functionalized surfaces with molecules that render the surface hydrophobic or hydrophilic. These molecules are designed to encourage or discourage metal colloid attachment.[24–30] Selective deposition of Pt and Pd can be accomplished using hexafluoroacetylacetonate complexes and metal–organic chemical vapor deposition (MOCVD).[31] By comparison, the method we report here requires no chemical etching and can be used to create a wide variety of geometrically distinct two-dimensional (2D) arrays of metal patterns without lithographically defining a different 2D master template for each new pattern.

In this work PDMS stamps were molded from commercial diffraction gratings with periods ranging from 417 nm (2400 grooves mm^{-1}) to 3.3 μm (300 grooves mm^{-1}) and used to print well-defined patterns of hydrophobic, passivating siloxane molecules on silica substrates. The stamped substrate is exposed to a metallization precursor, then to an electroless plating solution. This process results in directed electroless plating of the metal to form discrete metal structures over the entire surface. Because the surface is pre-patterned with passivated regions inert to metal deposition, the metal is directed only to the unstamped regions. This allows the formation of unconnected metal structures without any chemical etching steps. These metallic arrays are varied in size, separation and shape by using gratings of different periodicities and blaze angles as the stamp templates. A variety of well-defined geometric patterns have been fabricated and imaged using scanning probe, scanning electron, and optical microscopies.

Silver and gold gratings and 2D island arrays were fabricated on microscope slides cut into 1 cm^2 pieces to match the

[*] Prof. N. J. Halas, C. E. Moran, C. Radloff
Department of Chemistry and Department of Electrical and Computer Engineering, Rice University
6100 Main Street, Houston, TX 77005 (USA)
E-mail: halas@rice.edu

[**] The authors gratefully acknowledge support of this work from the Army Research Office MURI Program, the National Science Foundation, the Robert A. Welch Foundation, the Air Force Office of Scientific Research, and the Texas Advanced Technology Program.

  DOI: 10.1002/adma.200304507